Title: Authentication of Iberian dry-cured ham: new approaches by polymorphic fingerprint and ultrahigh resolution mass spectrometry.

Authors: L. Bayés-García[a], A. Tres[b], S. Vichi[c], T. Calvet[a], M.A. Cuevas-Diarte[a], R. Codony[b], J. Boatella[b], J. Caixach[d], S. Ueno[e], F. Guardiola[b*]

Affiliations:

[a] Departament de Cristal·lografia, Mineralogia i Dipòsits Minerals, Facultat de Geologia, Universitat de Barcelona, Martí i Franquès s/n, E-08028, Barcelona, Spain.

[b] Nutrition and Food Science Department – XaRTA – INSA, Faculty of Pharmacy, Universitat de Barcelona, Av. Joan XXIII s/n, E-08028 Barcelona, Spain.

[c] Nutrition and Food Science Department – XaRTA – INSA, Food and Nutrition Torribera Campus, Universitat de Barcelona, Av. Prat de la Riba 171, E-08921, Sta. Coloma de Gramenet, Spain.

[d] Mass Spectrometry Laboratory/Organic Pollutants, IDAEA-CSIC, Jordi Girona 18-26, E-08034 Barcelona, Spain.

[e] Graduate School of Biosphere Science, Hiroshima University, Higashi-Hiroshima, 739, Japan.

* Correspondence to: F. Guardiola (fguardiola@ub.edu); phone number: 34-93-4034842

Abstract: Foods with high added value, such as Iberian dry-cured products, are susceptible to fraud. Many attempts have been made to differentiate the commercial/quality categories of Iberian dry-cured hams by analytical determinations. However, as discrimination by such means is not fully reliable, legislation to prevent fraudulent practice is based on administrative controls and certification. Here, new analytical approaches based on ultrahigh resolution mass spectrometry (UHRMS) and crystallographic techniques applied to the lipid fraction, in combination with chemometrics, are studied. The results of the triacylglycerol profile determined by UHRMS and the fingerprint provided by the thermograms obtained by differential scanning calorimetry offer the promise of analytic discrimination of Iberian dry-cured ham categories. In addition, these determinations, in combination with chemometrics, may prove extremely useful to authenticate many foods containing high to moderate amounts of lipids.

Keywords: food authentication; polymorphic fingerprint; differential scanning calorimetry; synchrotron radiation; ultrahigh resolution mass spectrometry; chemometrics

Abbreviations: DSC, differential scanning calorimetry; FA, fatty acid; FWHM, full width at half maximum; GC-FID, gas chromatography-flame ionization detection; NIR, near-infrared; PCA, principal component analysis; PLS-DA, partial least squares–discriminant analysis; PSPC, position sensitive proportional counters; RDB, rings plus double bonds equivalents; RMSEcv, root mean square errors of cross-validation; SAXD small-angle X-ray diffraction; SR, synchrotron radiation; TAG, triacylglycerol; TOM,

thermo-optical polarized microscopy; UHRMS, ultrahigh resolution mass spectrometry; WAXD, wide-angle X-ray diffraction; XRD, X-ray diffraction.

1.Introduction

Iberian dry-cured ham is a traditional Spanish product that is greatly appreciated for its sensory characteristics and is associated with top quality gastronomy around the world. The economic impact of this sector is important; near to 9 million dry-cured hams and shoulders were produced in 2013 in Spain (RIBER, 2015). The socio-economic importance of pigs in Europe dates back to about 3000 BC, when the inhabitants of many farming villages cultivated a variety of crops, and raised cattle, sheep, goats and pigs (Waterbolk,1968). In Spain, during the pre-Roman period, the pig was represented in several objects and megalithic sculptures (4th-2nd century BC) by the Iberian Celtic peoples (Álvarez-Sanchís, 2008; Cerdeño, & Cabanes, 1994). Several Roman documents attest to the importance of pig breeding and the production of salted dry-hams in Hispania (Bello, 2008; Laguna, 1999). The pigs bred by the Celts and Romans might be the ancestors of the current local breed (Iberian).

Nowadays, Iberian pigs (pure breed or crossed with Duroc) are raised under different rearing systems and some of their dry-cured products (hams, shoulders and loins) are classified accordingly into three commercial categories with different quality characteristics (named *Cebo*, *Cebo de campo* and *Bellota*). Briefly, according to the Spanish legislation (Royal Decree 4/2014, 2014), the main differences between these categories are that *Bellota* products come from pigs with a final fattening period in oak forests (called *dehesas*) during which they eat exclusively acorns, grass and other natural resources of the pasture (minimum duration of this fattening period: 60 days;

minimum weight gain: 46 kg); while *Cebo de campo* and *Cebo* products come from pigs fed commercial feeds throughout their life, but in the case of *Cebo de campo* the animals roam in a pasture for at least 60 days prior to slaughter during which time they eat mainly commercial feeds. The rearing and feeding differences during the final fattening period yield different lipid deposition in adipose tissue and intramuscular fat, which influences the sensory quality of the dry-cured products (Tejeda, Gandemer, Antequera, Viau, & García, 2002). In addition, consumers greatly appreciate the sensory attributes of *Bellota* dry-cured products, which are much more expensive than the rest of Iberian dry-cured products. Moreover, livestock grazing in the *dehesa* contributes to preserving this valuable landscape and its extraordinary biodiversity. The pruning and reforesting of oaks are very important to maintain acorn production to feed Iberian pigs during the final fattening period and to preserve this ecosystem (Rodríguez-Estévez, et al., 2012). In addition, there is evidence that good management of agrosilvopastoral systems can improve their biodiversity (Benton, 2007; Boettcher, & Hoffmann, 2011). This fact adds value to *Bellota* products, which is increasingly appreciated by consumers.

Products with added value are susceptible to fraud, which might occur at different stages of the food chain, affecting the interest of all stakeholders: farmers, producers, retailers, regulatory bodies and consumers. To prevent fraudulent commercial practices, administrative controls and certifications are currently used, but analytical determinations to reliably differentiate these three categories of dry-cured products would be extremely beneficial. Several wet-chemical determinations such as those that assess the lipid composition of fat deposits (e.g., fatty acid or triacylglycerol composition) have been explored to date. However, these chemical determinations are

not able to completely discriminate samples in the different categories. Thus, in a recent study (García-Casco, Muñoz, & González, 2013) several analytical determinations were used to discriminate between the Iberian pig rearing/feeding systems (categories). After slaughtering, samples of subcutaneous adipose tissue (back fat) were taken close to the rump from 749 pigs coming from three seasons (2008-09, 2009-10 and 2010-11). Several determinations were carried in the adipose tissue samples: fatty acid (FA) composition determined by gas chromatography-flame ionization detection (GC-FID), near-infrared (NIR) signal, tocopherol composition determined by high-performance liquid chromatography-fluorescence detection, volatile compound fingerprint determined by head space-gas chromatography-mass spectrometry, triacylglycerol composition determined by GC-FID, stable isotopes (^{13}C) of different FA determined by gas chromatography-combustion-isotope ratio mass spectrometry, and neophytadiene determined by gas chromatography-mass spectrometry. The results from this comprehensive study show that these determinations are not able to completely discriminate samples in the different categories and that their discrimination ability is quite similar. Therefore, new analytical approaches to authenticating Iberian dry-cured products are necessary. State-of-the-art chemometric strategies in food authentication rely on finding a pattern in raw analytical data characteristic of the authentic product (Bosque-Sendra, Cuadros-Rodriguez, Ruiz-Samblas, & De la Mata, 2012). This unique pattern is used as a fingerprint of the authentic product to distinguish it from non-authentic products. In this work, we study the potential of electrospray ultrahigh resolution mass spectrometry (ESI-UHRMS) and some crystallographic techniques, in combination with chemometrics, to authenticate Iberian dry-cured hams. The performances achieved by recent MS instrumentation make direct UHRMS a promising novel approach to food authentication, although few

applications are yet reported (Hrbek, Vaclavik, Elich, & Hajslova, 2014; Roullier-Gall, Boutegrabet, Gougeon, & Schmitt-Kopplin, 2014). Crystallographic techniques, such as laboratory-scale X-ray diffraction (XRD) or XRD using a synchrotron radiation source (SR-XRD), differential scanning calorimetry (DSC) and thermo-optical polarized microscopy (TOM) have been widely used to study the polymorphism of edible fats and oils, in order to characterize their physical properties (e.g., melting, morphology, rheology, and texture) (Larsson, Quinn, Sato, & Tiberg, 2006). However, these crystallographic techniques have rarely been used in food authentication.

Therefore, our main objectives were to establish whether DSC thermograms and the triacylglycerol (TAG) profile determined by direct ESI-UHRMS, in combination with chemometrics, are useful to authenticate Iberian dry-cured hams, and to compare their reliability with that of a classical method: the FA composition. The fingerprint approach was used for DSC thermograms. Moreover, in an attempt to characterize the crystallization, transformation and melting processes, DSC data were complemented with TOM, XRD and SR-XRD.

To that end, 10 authentic *Cebo* and 10 authentic *Bellota* Iberian dry-cured ham samples were used as a first approach to Iberian ham authentication, since they are the two least similar ham categories; thus methods that failed at this point would be of no use in authentication. On the contrary, methods useful in this model could be also useful to authenticate many foods containing high to moderate amounts of lipids, such as other foods of animal origin. Therefore, this is a proof of concept to study the capability of new analytical approaches to discriminate between Iberian dry-cured ham categories.

2. Materials and methods

2.1. Chemicals

Dichloromethane and methanol used for TAG determination by ESI-UHRMS were of HPLC/MS grade (Merck, Darmstadt, Germany). Nitrogen (Alphagaz^{TM}, purity 99.999%, Air Liquide) was used in the Orbitrap-Exactive as nebulization gas. The rest of reagents used in the analytical procedures were of analysis grade.

2.2. Lipid extraction

Fifty three g of subcutaneous adipose tissue from each ham sample were grinded 3 times for 10 seconds at 7000 rpm (Retsch GM 200 knife mill, Haan, Germany). Seven to eight g of ground sample were weighed in 32 x 210 mm tubes. Subsequently, 32 mL of petroleum ether 40-60 ºC were added and the mixture was homogenized for 30 s at 19,000 rpm using a Polytron PT 3,100 (Kinematica, Lucerne, Switzerland). The extract was decanted and filtered through Whatman nº4 filter paper into a 50 mL screw-capped tube and the residue was re-extracted in the same way with 33 mL of petroleum ether. The second filtrate was recovered in another screw-capped tube. Then, 10 mL of 1 % (w/v) aqueous sodium chloride were added to each tube. Both tubes were gently shaken and centrifuged at 400 x g for 15 min. Both petroleum ether extracts were filtered through anhydrous sodium sulfate (using a Whatman nº1 filter paper), which was then washed twice with 10 mL of the solvent. The filtrate was recovered in a round-bottom flask and the solvent was evaporated nearly to dryness in a vacuum rotatory evaporator at 35ºC. Solvent evaporation was completed by placing the round-bottom flask in a vacuum dessicator at 10 mmHg for 30h. The flask was briefly heated at 45 ºC and once the lipid extract was homogeneous it was distributed in various vials, filling the

176 headspace with nitrogen. Then, the vials were stored at -20ºC until all the
177 determinations were carried.
178
179 *2.3. Fatty acid determination*
180 After FA methyl ester preparation, the FA composition of the lipid extracts was
181 determined using GC-FID (Bou, Codony, Tres, Baucells, & Guardiola, 2005). Each
182 sample was methylated in duplicate.
183
184 *2.4. Triacylglycerol determination by electrospray ultrahigh resolution mass*
185 *spectrometry*
186 *2.4.1. Sample preparation*. 30 mg of fat sample were dissolved in 3 mL of
187 dichloromethane:methanol 7:3 (v/v), then diluted with the same solvent to a
188 concentration of 0.01 mg/L (w/v). Before the last dilution NaCl was added as
189 cationization agent. Each sample was injected in duplicate.
190 *2.4.2. Orbitrap-Exactive Mass Spectrometry*. Direct injection analysis of 5 µL of the
191 samples was carried out with an Orbitrap-Exactive (Thermo Fisher Scientific, Bremen,
192 Germany), according to Vichi, Cortés-Francisco, and Caixach (2012). The ionization
193 was performed by an electrospray source (H-ESI II). The LC system consisted of a
194 Surveyor MS Plus pump (Thermo Fisher Scientific, San Jose, California). The mobile
195 phase was methanol:dichloromethane 80:20 (v/v) at 50 µL/min.
196 Mass spectra were acquired in full scan positive ionization mode by applying the
197 following parameters: spray voltage 3.00kV, capillary voltage 37V, tube lens 150V and
198 skimmer voltage 40V. The sheath gas flow rate was set at 35 au (arbitrary units) and the
199 aux gas flow rate was 5 au. Capillary and heater temperatures were fixed at 400 ºC and
200 30 ºC, respectively. The mass range was set to *m/z* 200-1200. The automatic gain

control was used to fill the C-trap (ultimate mass accuracy mode, $5x10^5$ ions). Ultrahigh resolving power defined as R: 100,000 (*m/z* 200, FWHM) was set.

The mass peaks considered were single positive charged sodium molecular ions with relative intensities ≥0.1% and absolute intensity $>10^3$. These peaks were exported to peak lists and from these lists feasible elemental formulae were generated. In order to obtain a limited list of possible candidates from a mass measurement, restrictive criteria were set to generate reliable elemental formulae: C ≤ 200, H ≤ 100, O = 6, Na=1 and RDB (rings plus double bonds equivalents): 2.5-11.5. The molecular formulae calculation was performed with Xcalibur 2.1 (Thermo Fisher Scientific, Bremen, Germany) and the posterior analysis of the data was done using excel files.

2.5. Differential scanning calorimetry, X-ray diffraction and thermo-optical polarized microscopy analysis

DSC analysis was conducted at atmospheric pressure using a Perkin-Elmer DSC-7 calorimeter, by cooling the melted lipid extracts from 65ºC to -80ºC at $2ºC \cdot min^{-1}$ and then heating them to 65ºC at the same rate. Samples (9.0 to 9.4mg) were weighed into 50 μL aluminium pans, and covers were sealed into place. Three independent DSC measurements were made for each sample.

Laboratory-scale and synchrotron radiation XRD experiments were carried out to determine the polymorphic crystallization and transformation processes observed in the DSC thermograms. One sample of each category was analyzed by using the two techniques. Laboratory-scale XRD was performed by a PANalytical X'Pert Pro MPD powder diffractometer equipped with a Hybrid Monochromator and an X'Celerator Detector. The equipment also included an Oxford Cryostream Plus 220 V (temperature

80−500 K) that allows heat/cool the sample at 2ºC·min^{-1}. The sample was introduced in a 1 mm-diameter Lindemann glass capillary that was rotated around its axis during the experiment to minimize preferential orientation of the crystallites. SR-XRD with simultaneous measurements of small- and wide-angle XRD (SAXD and WAXD) were carried out at the BL-6A of the Photon Factory synchrotron radiation facility in Tsukuba, Japan. For this beamline a double-focusing camera operated at a wavelength of 0.15 nm and the X-ray scattering data were simultaneously collected by position sensitive proportional counters (PSPC) (Rigaku Co., PSPC-10), SAXD and WAXD. Each temperature program was controlled by a Linkam THMSF-600 stage and a 2-mm-thick sample was placed in an aluminum sample cell with Kapton film windows.

TOM images were obtained on a Linkam THMSG-600 stage mounted to a Nikon Eclipse 50iPol Microscope. The sample was placed on a 7 mm quartz coverslip and encased within a pure Ag lid to ensure a uniform temperature. An LNP liquid nitrogen cooling system and a TMS94 temperature controller were used. Images were captured with a Nikon Digital Camera DXM1200F and Linksys32 Software.

More details of the methods used for DSC, XRD, SR-XRD and TOM analysis are given elsewhere [Bayés-García, Calvet, Cuevas-Diarte, Ueno, & Sato, 2011; Bayés-García, Calvet, Cuevas-Diarte, Ueno, & Sato, 2013).

2.6. Chemometrics

Chemometrics was applied to the DSC, TAG and FA data independently. Software used was SIMCA v 13.0 (Umetrics AB, Umeå, Sweden). First, principal component analysis (PCA) was developed to explore the data in order to reveal the presence of

outliers and natural clustering of samples. No outlier samples were found, and natural clustering was observed for *Bellota* and *Cebo* samples (data not shown). Then, classification models were developed to discriminate the *Cebo* from the *Bellota* dry-cured ham samples based on partial least squares–discriminant analysis (PLS-DA). The PLS-DA model implied that y values were set to 1 for one of the categories (i.e., *Bellota*) and to 0 for the other category (i.e., *Cebo*). The cut-off value was set at 0.5; thus, when the predicted value was above 0.5, the sample was classified as *Bellota*, and when the predicted value was below 0.5, the sample was classified as *Cebo*. The models were fitted and validated by leave 10%-out cross-validation (analytical replicates were left out in the same cross-validation group). Model performance was evaluated by the % of correctly identified samples and by the root mean square errors of cross-validation (RMSEcv). Prior to model development, several data pre-treatment and pre-processing techniques were applied. Derivatives (1^{st} and 2^{nd}), in combination (or not) with variable centering (around the mean, UV procedure in SIMCA software; or around 0, UVN procedure in SIMCA software), and scaling to unit variance were applied with the DSC data sets. Variable centering and scaling to unit variance (UV procedure in SIMCA software) were applied to the TAG and FA data sets.

3. Results and discussion

Important differences between the two Iberian ham categories were revealed by the DSC cooling and heating thermograms of the lipid extracts. The variations observed were primarily based on the position and relative intensity of the corresponding exothermic and endothermic signals. These differences can be appreciated in the typical DSC cooling and heating curves of the two ham categories (Fig. 1). All samples

belonging to the same Iberian ham category exhibited the same thermal profile and the DSC curves for three independent measurements for each sample were almost identical in all cases. This was confirmed by further evaluation applying PLS-DA to two selected data ranges of the DSC thermograms: from 25ºC to -45ºC (cooling thermogram) and from -30ºC to 40ºC (heating thermogram). The PLS-DA revealed that after proper raw data pre-processing (1^{st} derivative and scaling to unit variance for cooling data; 1^{st} derivative for heating data) both cooling and heating thermograms successfully discriminated *Cebo* and *Bellota* samples (Fig. 2) with 100% of the samples correctly assigned to their category.

Synchrotron radiation and laboratory-scale XRD experiments were performed, as a function of temperature, on *Cebo* and *Bellota* samples, in order to clarify the polymorphic crystallization and transformation processes observed in the DSC thermograms. The results obtained via the two techniques were essentially the same and Fig. 3 displays, as an example, the SR-XRD data obtained for typical *Cebo* (C1) and *Bellota* (B1) samples. Long-spacing values were used to determine the chain-length structures (double, 2L or triple, 3L); while short-spacing values permitted us to identify the polymorphic forms. In general, the most commonly encountered polymorphic forms of TAGs are the α form, which is defined by a hexagonal subcell (H), the β' form, with an orthorhombic perpendicular subcell ($O_{\perp}$) and the β form with a typical triclinic parallel subcell ($T_{//}$) (Larsson, Quinn, Sato, & Tiberg, 2006).

The two samples exhibited highly complex but similar SR-XRD patterns when they were subjected to the same thermal program as that followed by DSC. By cooling the melted samples, both C1 and B1 showed the occurrence of an initial sub-α-2L form

and, soon after, a β'-3L form crystallized. These two crystallizations corresponded to the first set of exothermic peaks that appeared from 20ºC to -5ºC in the DSC cooling thermogram (Fig. 1). On further cooling, a newly formed β'-2L form was detected, which corresponded to the second set of crystallization peaks from -10ºC to -40ºC. Thus, the polymorphic crystallization of the two categories became highly similar. However, according to the DSC cooling curves, polymorphic crystallization occurred at a higher temperature in the C1 sample than in the B1 sample, which may be related to the more saturated nature of *Cebo* samples, compared to *Bellota* samples. The results agree with those observed by inspecting the first PLS-DA loading of DSC cooling (Fig. 4). The temperature ranges from 16.4ºC to 14.5ºC, from 9.3ºC to 7.1ºC and from -17.2ºC to -26.8ºC were the most significant for the identification of *Cebo* samples. In contrast, the PLS-DA indicates that the most important ranges for identifying *Bellota* samples were from 14.5ºC to 9.3ºC, from 7.1ºC to -1.4ºC, from -8.5ºC to -17.2ºC and from -26.9ºC to -37.7ºC.

As to the heating treatment, most significant differences between the two categories were detected at the last stage of the process, especially according to the SR-SAXD data. These main variations observed were based on the sequence of melting processes of the different polymorphic forms, which again may be caused by the more saturated composition of *Cebo* samples (see Tables 1 and 2 for FA and TAG composition). As shown in the enlarged image in Fig. 3, for sample C1, the first melting process corresponded to sub-α-2L form (4.8 nm), and it was followed by the melting of β'-3L (3.5 nm) and β'-2L (4.4 nm) forms. In contrast, for sample B1, β'-2L melted first, and on further heating, sub-α-2L and β'-3L forms melted. In general, for a given TAG, 3L forms exhibit higher melting point than 2L forms. In the *Cebo* sample, 2L forms melted

at higher temperatures than 3L forms, which may indicate that the 2L form comes from more saturated TAGs than that with 3L structure. On the contrary, in the *Bellota* sample, the last melting form exhibited a 3L structure. Again, these results agree with the importance of the temperature range between 30ºC and 34.2ºC in the PLS-DA model of DSC heating data for the discrimination of *Bellota* samples; and the ranges from 22.0ºC to 29.8ºC and from -6.0ºC to 0.2ºC for the discrimination of *Cebo* samples (Fig. 4). Although the cooling and heating PLS-DA models correctly classified all the samples, the RMSEcv showed that the model based on heating data was the more promising approach (cooling: RMSEcv = 0.331; heating: RMSEcv = 0.287).

The same thermal treatment was applied to the TOM analysis in order to visualize the crystallization and melting behavior of *Cebo* and *Bellota* samples (Fig. 5). Using this technique, it was also possible to observe some differences in the crystallization behavior and crystal morphology of the lipid extracts from the two Iberian ham categories. Two different crystallization steps could easily be distinguished when cooling *Cebo* samples, whereas *Bellota* samples exhibited a more gradual crystallization process. As for the crystal morphology, more aggregated, larger and thicker crystals were obtained from the melted *Cebo* lipid extract; while separated spherulites, with an average diameter of approximately 10 μm, could easily be observed in the TOM micrographs of the *Bellota* lipid extract.

Direct ESI-UHRMS of dry-cured ham fat allowed fast and reliable determination of nearly fifty compounds with molecular formulae attributable to TAG species with CN from C27 to C56, and abundances from 0.01 to 31.94 % (Table 2). Major TAGs were C55H102O6Na (POO/PSL/PoSO), C55H104O6Na (PSO/PoSS), C55H100O6Na

(POL/PSLn/PoOO/PoSL) and C57H104O6Na (OOO/SOL/SSLn). In general, Cebo Iberian dry-cured hams showed higher amounts of diunsaturated TAGs than Bellota samples (44.04 ± 0.69 % versus 42.12 ± 1.13 %, respectively), while the latter were richer in triunsaturated (28.45 ± 1.5 % versus 26.32 ±0.80 %) and tetraunsaturated TAGs (9.18 ± 0.87 % versus 8.33 ± 0.56 %), as proved by Student's t-test (Table 2). In addition, the detailed profiles obtained by direct ESI-UHRMS offered several signals attributable to minor TAGs providing information to the classification model. The amounts of most of them showed significant differences between Cebo and Bellota Iberian dry-cured hams (Table 2).

TAGs composition in combination with chemometrics also offered a highly promising scenario for the discrimination of *Cebo* and *Bellota* Iberian dry-cured hams (Fig. 2). The RMSEcv of the TAG composition (RMSEcv = 0.236) was slightly lower than that of the PLS-DA for the DSC heating thermogram; while that of the FA approach was even lower (RMSEcv = 0.141). The TAG and FA compositions achieved 100% correct classification of the samples during cross-validation. Among the most important TAGs to differentiate the *Bellota* category (Table 2) were those corresponding to the molecular formulae: $C_{57}H_{104}O_6Na$, $C_{59}H_{108}O_6Na$ and $C_{57}H_{102}O_6Na$, attributable to the TAGs: OOO/SOL/SSLn, OOG/OLA/SLG and OOL/SLL/SOLn, respectively (with the abbreviations, P: palmitic (C16:0); Po: palmitoleic (C16:1n-9); O: oleic (C18:1n-9); S: stearic (C18:0); L: linoleic (C18:2n-6); Ln: linolenic (C18:3n-3); G: gondoic (C20:1n-9); and A: arachidic (C20:0)). The FAs driving the discrimination of the *Bellota* category were those belonging to the n-9 monounsaturated FA series, such as: C16:1n-9, C18:1n-9 and C20:1n-9 (Table 1).

4. Conclusions

Here we show that the combination of chemometrics and fat crystallization, transformation and melting data obtained by DSC is a promising methodology to obtain a polymorphic fingerprint that can be used to discriminate between Cebo and Bellota dry-cured Iberian ham. The ultimate aim of this study will be to evaluate the polymorphic fingerprint and the TAG composition determined by UHRMS as tools to discriminate the three Iberian ham categories, comparing their performance with that of the FA composition. The next steps towards their full application as authentication tools will be to increase the number of samples, include samples from the third category and test the performance of the models with additional sources of natural variability such as interyear variability. Moreover, the increase in the number of samples would also allow external validation of the PLS-DA models using a set of samples that were not used in model fitting. However, the results obtained up to now show that DSC and TAG composition determined by UHRMS, in combination with chemometrics, may become very useful and straightforward techniques to combat food fraud.

Acknowledgements

The authors acknowledge the financial support of the Ministerio de Economía y Competitividad through Project MAT2011-27225, and through the post-doctoral research grants awarded to A. Tres (Juan de la Cierva Program, JCI-2012-13412) and to S. Vichi (Ramón y Cajal Program, RYC-2010-07228).

References

Álvarez-Sanchís, J.R. (2008). *Los señores del ganado: arqueología de los pueblos prerromanos en el occidente de Iberia*. Tres Cantos, Spain: Ediciones Akal.

Bayés-García, L., Calvet, T., Cuevas-Diarte, M.A., Ueno, S., & Sato, K. (2011). *In situ* synchrotron radiation X-ray diffraction study of crystallization kinetics of polymorphs of 1,3-dioleoyl-2-palmitoyl glycerol (OPO). *CrystEngComm, 13,* 3592-3599.

Bayés-García, L., Calvet, T., Cuevas-Diarte, M.A., Ueno, S., & Sato, K. (2013). Crystallization and transformation of polymorphic forms of trioleoyl glycerol and 1,2-dioleoyl-3-*rac*-linoleoyl glicerol. *J. Phys. Chem. B., 117,* 9170-9181.

Bello, J. (2008). *Jamón curado: aspectos científicos y tecnológicos*. Madrid, Spain: Diaz de Santos, (Chapter 5).

Benton, T.G. (2007). Managing farming's footprint on biodiversity. *Science, 315,* 341-342.

Boettcher, P.J., & Hoffmann, I. (2011). Protecting indigenous livestock diversity. *Science, 334,* 1058.

Bosque-Sendra, J.M., Cuadros-Rodriguez, L., Ruiz-Samblas, C., & De la Mata, A.P. (2012). Combining chromatography and chemometrics for the characterization and authentication of fats and oils from triacylglycerol compositional data-A review. *Anal. Chim. Acta, 724,* 1-11.

Bou, R., Codony, R., Tres, A., Baucells, M.D., & Guardiola, F. (2005). Increase of geometrical and positional fatty acid isomers in dark meat from broilers fed heated oils. *Poult. Sci., 84,* 1942-1954.

Cerdeño, M.L., & Cabanes, E. (1994). The symbolism of the boar in the Celtic peninsular area. *Trabajos Prehist., 51,* 103-119.

García-Casco, J.M., Muñoz, M., & González, E. (2013). Predictive ability of the feeding system in Iberian pig by means of several analytical methods. *Grasas y Aceites, 64 (special issue),* 191-200.

Hrbek, V., Vaclavik, L., Elich, O., & Hajslova, J. (2014). Authentication of milk and milk-based foods by direct analysis in real time ionizationehigh resolution mass spectrometry (DARTeHRMS) technique: A critical assessment. *Food Control, 36*, 138-145.

Laguna, E. (1999). El cerdo ibérico y los encinares un apoyo mutuo multisecular. In A. Josemaria-Bastida, & M.D. García-Cachán (Eds.), *I Jornadas sobre el cerdo ibérico y sus productos* (pp. 11-17). Guijuelo, Spain: Estación Tecnológica de la Carne de Castilla y León.

Larsson, K., Quinn, P., Sato, K., & Tiberg, F. (2006). *Lipids: Structure, Physical Properties and Functionality*, Bridgwater, England: The Oily Press.

RIBER (Information Register on Independent Iberian Control Bodies). Iberian Round Table. Ministerio de Agricultura, Alimentación y Medio Ambiente. 2013 data, access on the 4-28-2015. http://www.magrama.gob.es/app/riber/Publico/BuscadorProductosCertificados.aspx .

Rodríguez-Estévez, V., Sánchez-Rodríguez, M., Arce, C., García, A. R., Perea, J. M., & Gómez-Castro, A.G. (2012). Consumption of acorns by finishing Iberian pigs and their function in the conservation of the dehesa agroecosystem. In M. L. Kaonga (Ed.), *Agroforestry for biodiversity and ecosystem services - science and practice* (pp. 1-22). Rijeka, Croatia: InTech.

Roullier-Gall, C., Boutegrabet, L., Gougeon, R.D., & Schmitt-Kopplin, P. (2014). A grape and wine chemodiversity comparison of different appellations in Burgundy: vintage vs terroir effects. *Food Chem., 152,* 100-107.

Royal Decree 4/2014. (2014). Approves the quality standards for the Iberian meat, ham, shoulder and loin. *BOE, No. 10 (January 11th, 2014),* 1569-1585.

Tejeda, J.F., Gandemer, G., Antequera, T., Viau, M., & García, C. (2002). Lipid traits of muscles as related to genotype and fattening diet in Iberian pigs: total intramuscular lipids and triacylglycerols. *Meat Sci., 60,* 357-363.

Vichi, S., Cortés-Francisco, N., & Caixach, J. (2012). Ultrahigh resolution mass spectrometry and accurate mass measurements for high-throughput food lipids profiling. *J. Mass Spectrom., 47,* 1177-1190.

Waterbolk, H.T. (1968). Food production in prehistoric Europe. *Science, 162,* 1093-1102.

463

464

465

466 **Fig. 1.** Typical DSC thermograms of *Cebo* (sample C1) and *Bellota* (sample B1)
467 samples obtained when cooled and heated at 2ºC·min^{-1}. A) DSC cooling curves. B)
468 DSC heating curves.

469 **Fig. 2.** PLS-DA scores plot: first two factors of the PLS-DA models based on (A) the
470 cooling thermogram (from 25ºC to -45ºC; data correspond to 1st derivative and scaling
471 of variables to unit variance, 3 measurements per sample); (B) heating thermogram
472 (from -30ºC to 40ºC; data correspond to 1st derivative of variables, 3 measurements per
473 sample); (C) triacylglycerol composition by UHRMS (data correspond to variable
474 centering and scaling to unit variance, averages of two determinations per sample); and
475 (D) fatty acid composition (data correspond to variable centering and scaling to unit
476 variance, averages of two determinations per sample).

477 **Fig. 3.** SR-SAXD and SR-WAXD patterns of C1 and B1 samples.

478 **Fig. 4.** PLS-DA loadings plot: first factors of the models based on (A) the cooling
479 thermogram (from 25ºC to -45ºC; data correspond to 1st derivative and scaling of
480 variables to unit variance); and (B) heating thermogram (from -30ºC to 40ºC; data
481 correspond to 1st derivative of variables).

482 **Fig. 5.** Thermo-optical polarized microscopy images obtained when *Cebo* and *Bellota*
483 samples were cooled and heated at 2ºC·min^{-1}.

484

485

486

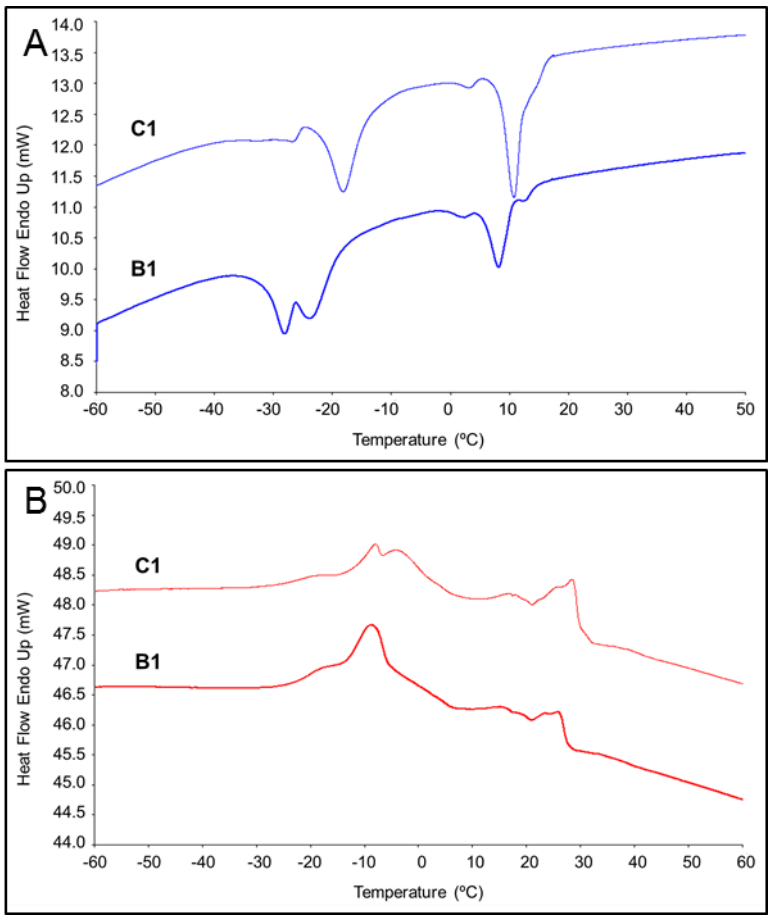

Fig. 1. Typical DSC thermograms of *Cebo* (sample C1) and *Bellota* (sample B1) samples obtained when cooled and heated at 2ºC·min^{-1}. A) DSC cooling curves. B) DSC heating curves.

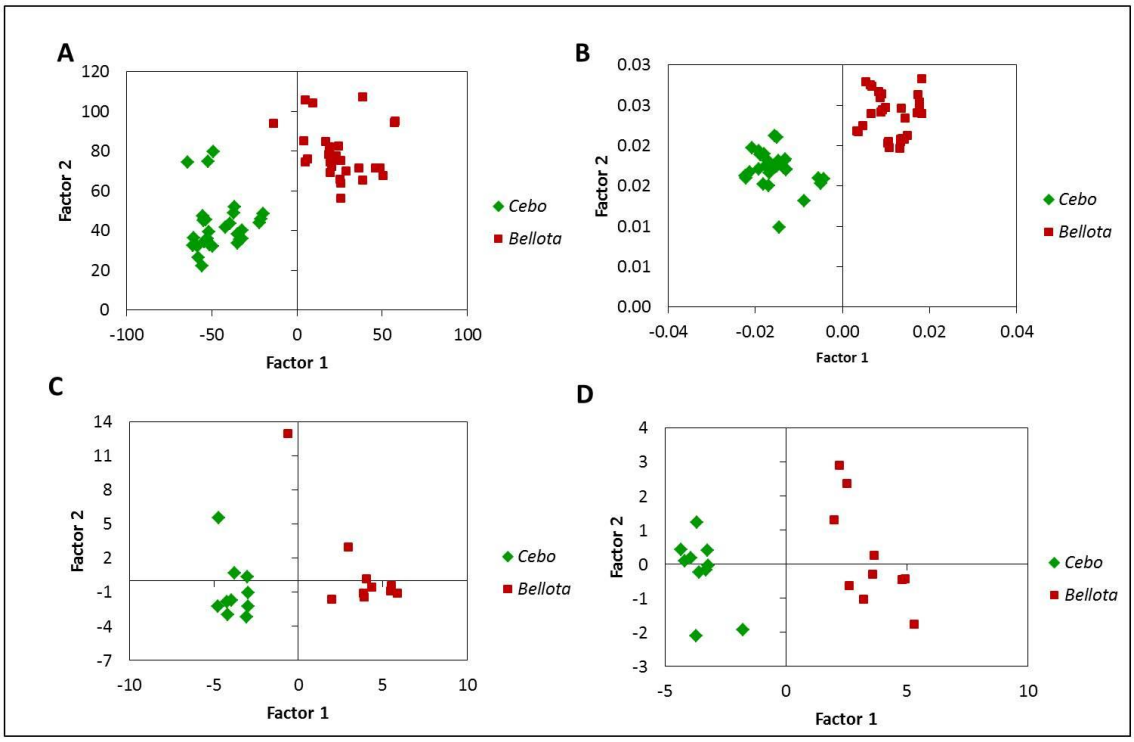

Fig. 2. PLS-DA scores plot: first two factors of the PLS-DA models based on (A) the cooling thermogram (from 25ºC to -45ºC; data correspond to 1st derivative and scaling of variables to unit variance, 3 measurements per sample); (B) heating thermogram (from -30ºC to 40ºC; data correspond to 1st derivative of variables, 3 measurements per sample); (C) triacylglycerol composition by UHRMS (data correspond to variable centering and scaling to unit variance, averages of two determinations per sample); and (D) fatty acid composition (data correspond to variable centering and scaling to unit variance, averages of two determinations per sample).

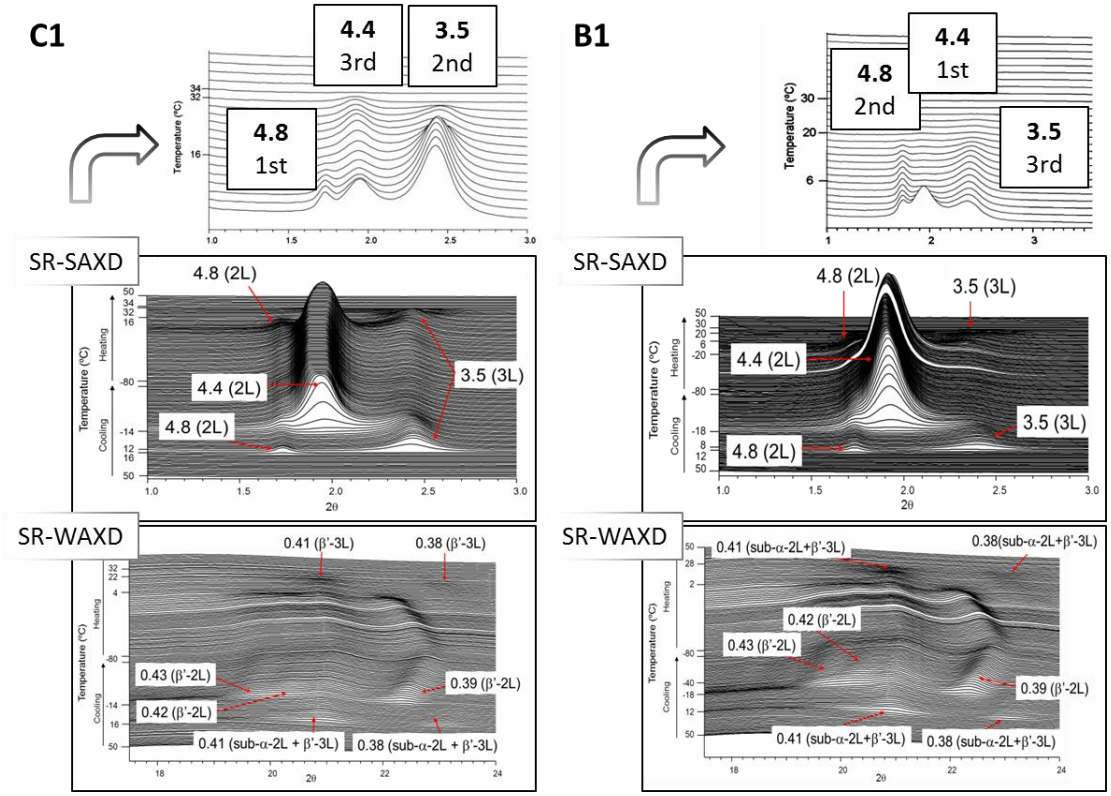

Fig. 3. SR-SAXD and SR-WAXD patterns of C1 and B1 samples.

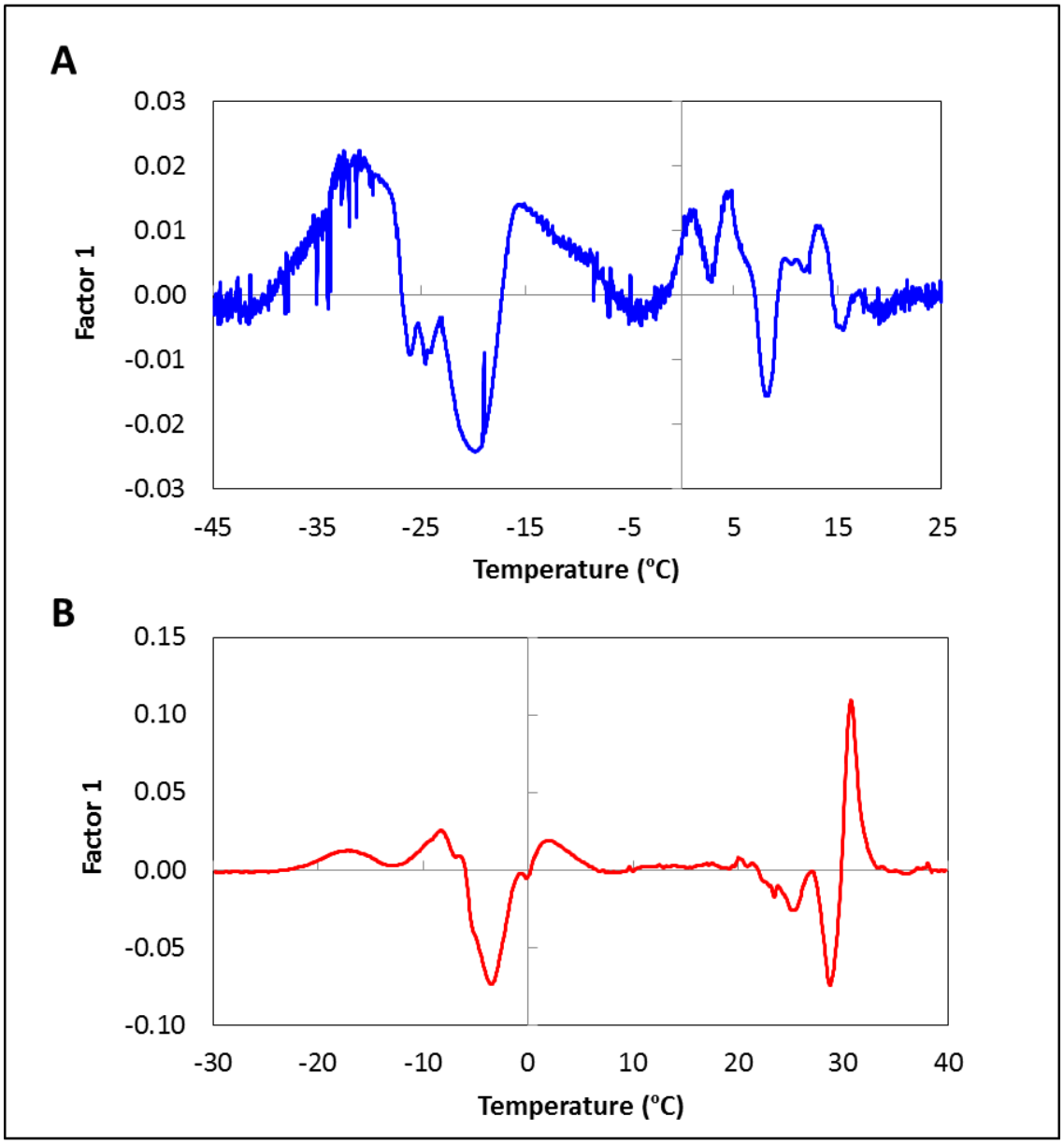

Fig. 4. PLS-DA loadings plot: first factors of the models based on (A) the cooling thermogram (from 25ºC to -45ºC; data correspond to 1st derivative and scaling of variables to unit variance); and (B) heating thermogram (from -30ºC to 40ºC; data correspond to 1st derivative of variables).

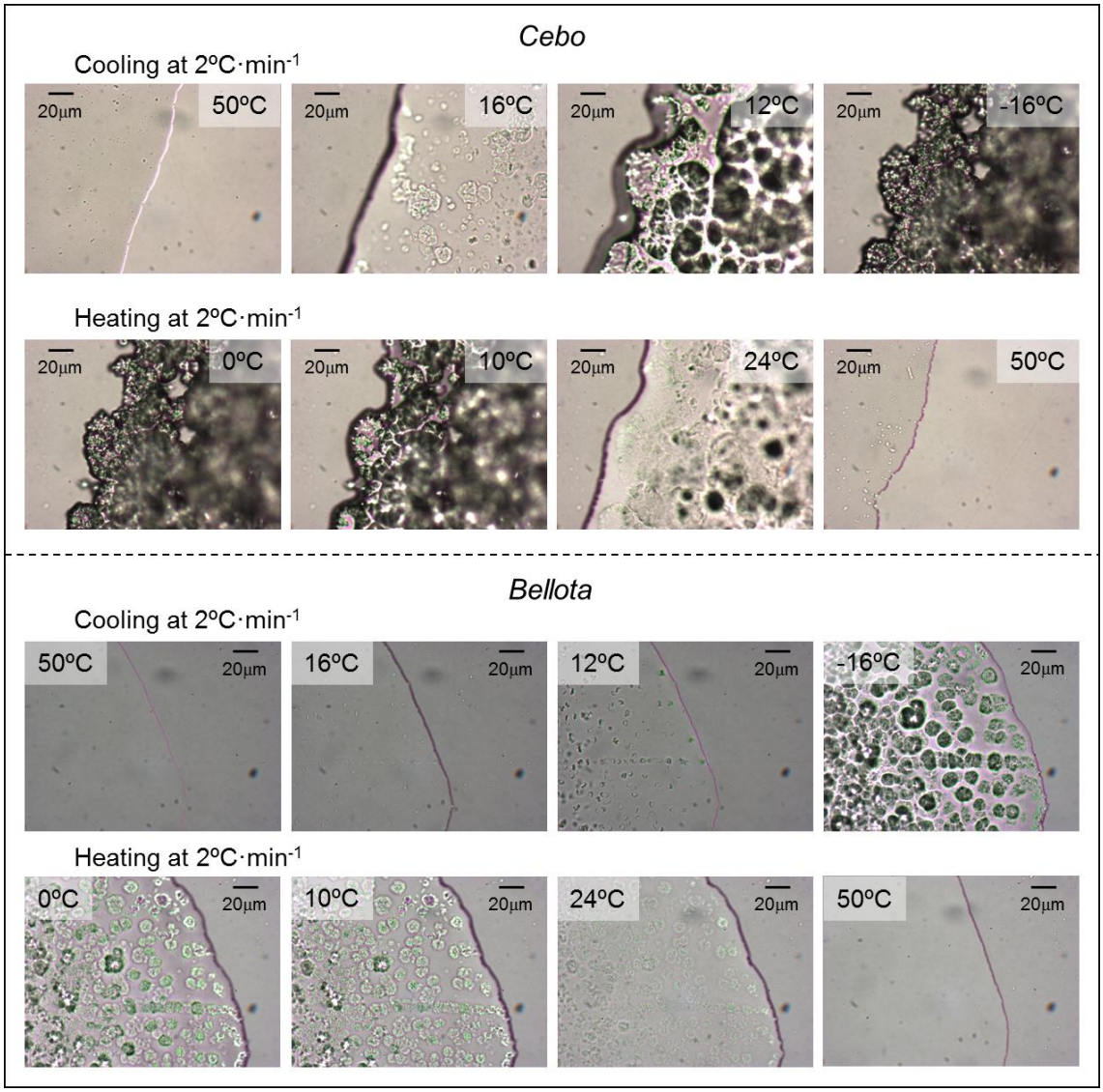

Fig. 5. Thermo-optical polarized microscopy images obtained when *Cebo* and *Bellota* samples were cooled and heated at 2ºC·min^{-1}.

543 **Table 1.** Fatty acid composition (peak area normalization expressed in %) of *Cebo* and *Bellota*

544 samples.

Fatty acid	*Cebo* (n=10)[a]		*Bellota* (n=10)[a]		*p*[b]	Loading[c]
	Mean	SD	Mean	SD		
C10:0	0.05	0.004	0.04	0.003	0.000	-0.262
C12:0	0.07	0.004	0.06	0.011	0.009	-0.159
C14:0	1.46	0.060	1.22	0.097	0.000[d]	-0.235
C15:0	0.06	0.006	0.05	0.006	0.000	-0.228
C16:0	23.47	0.521	20.67	0.832	0.000	-0.252
C17:0	0.34	0.028	0.29	0.042	0.003	-0.176
C18:0	10.88	0.504	9.64	0.711	0.000	-0.203
C20:0	0.18	0.017	0.18	0.014	0.913	0.007
C24:0	0.07	0.023	0.04	0.011	0.003[d]	-0.184
SFA	**36.58**	**0.830**	**32.17**	**1.365**	**0.000**	
C16:1n-9	0.34	0.017	0.42	0.021	0.000	0.251
C16:1n-7	2.55	0.177	1.89	0.254	0.000	-0.239
C17:1n-7	0.35	0.029	0.27	0.051	0.000	-0.200
C18:1n-9	44.89	0.437	52.08	1.375	0.000[d]	0.269
C18:1n-7	3.59	0.166	2.74	0.339	0.000[d]	-0.239
C20:1n-9	1.20	0.108	1.36	0.127	0.006	0.164
C24:1n-9	0.07	0.010	0.04	0.015	0.000	-0.201
MUFA	**52.99**	**0.687**	**58.81**	**1.045**	**0.000**	
C18:2n-6	8.40	0.467	7.42	0.412	0.000	-0.212
C20:2n-6	0.56	0.045	0.48	0.050	0.002	-0.180
C20:3n-6	0.07	0.007	0.06	0.008	0.005	-0.168
C20:4n-6	0.12	0.011	0.10	0.014	0.000	-0.205
n-6 PUFA	**9.15**	**0.505**	**8.06**	**0.468**	**0.000**	
C18:3n-3	0.55	0.039	0.45	0.046	0.000	-0.217
C20:3n-3	0.12	0.018	0.10	0.015	0.022	-0.142
C20:5n-3	0.02	0.009	0.02	0.005	0.061	-0.119
n-3 PUFA	**0.69**	**0.047**	**0.56**	**0.059**	**0.000**	
PUFA	**9.84**	**0.550**	**8.62**	**0.519**	**0.000**	
trans 18:1	0.59	0.092	0.40	0.079	0.000	-0.214

545

546 Abbreviations: SFA, saturated fatty acids; MUFA, monounsaturated fatty acids; PUFA,

547 polyunsaturated fatty acids.

[a] 10 samples per group were determined in duplicate, the averages of the duplicates were used in the calculations.

[b] P values were obtained by Student's t-test (IBM SPSS statistics v.20), assuming equality of variances according to Levene's test ($p>0.05$).

[c] Loading in the first factor of the PLS-DA model developed with fatty acid data (SIMCA, Umetrics AB).

[d] P values were obtained by Student's t-test, assuming non-equality of variances according to Levene's test ($p<0.05$).

575 **Table 2**. Triacylglycerol (TAG) composition (normalized ion abundances expressed in %) of *Cebo* and *Bellota*
576 samples.

TAG molecular Formula	*m/z* $[M+Na]^+$	Δ (ppm)[a]	CN/DB[b]	*Cebo* (n=10)[c]		*Bellota* (n=10)[c]		*p*[d]	Loading[e]
				Mean	SD	Mean	SD		
$C_{37}H_{70}O_6Na$	633.5065	-0.15	C34:0	0.10	0.021	0.12	0.047	0.144 [f]	0.094
$C_{49}H_{94}O_6Na$	801.6943	1.1	C46:0	0.11	0.092	0.11	0.132	0.866	-0.011
Saturated				**0.21**	**0.102**	**0.23**	**0.158**	**0.781**	
$C_{30}H_{54}O_6Na$	533.3813	-0.67	C27:1	0.04	0.022	0.02	0.023	0.078	-0.110
$C_{36}H_{66}O_6Na$	617.4752	-0.69	C33:1	0.01	0.009	0.05	0.042	0.020 [f]	0.149
$C_{37}H_{68}O_6Na$	631.4908	0.19	C34:1	0.13	0.030	0.15	0.047	0.327	0.063
$C_{39}H_{72}O_6Na$	659.5221	0.37	C36:1	0.09	0.019	0.18	0.064	0.002 [f]	0.187
$C_{45}H_{84}O_6Na$	743.616	1	C42:1	0.05	0.023	0.02	0.040	0.061	-0.116
$C_{47}H_{88}O_6Na$	771.6473	0.8	C44:1	0.13	0.050	0.11	0.099	0.588	-0.035
$C_{49}H_{92}O_6Na$	799.6786	0.91	C46:1	0.25	0.119	0.23	0.213	0.842	-0.013
$C_{50}H_{94}O_6Na$	813.6943	0.71	C47:1	0.12	0.143	0.15	0.241	0.730	0.022
$C_{51}H_{96}O_6Na$	827.7099	0.87	C48:1	0.91	0.129	0.78	0.271	0.202	-0.081
$C_{52}H_{98}O_6Na$	841.7256	0.84	C49:1	0.16	0.098	0.15	0.186	0.922	-0.006
$C_{53}H_{100}O_6Na$	855.7412	1.24	C50:1	4.75	0.235	4.05	0.509	0.001	-0.186
$C_{54}H_{102}O_6Na$	869.7569	1.69	C51:1	0.37	0.051	0.25	0.074	0.000	-0.197
$C_{55}H_{104}O_6Na$	883.7725	1.55	C52:1	11.76	0.717	11.42	1.385	0.000 [f]	-0.043
Monounsaturated				**18.77**	**1.239**	**17.55**	**2.115**	**0.135**	
$C_{37}H_{66}O_6Na$	629.4752	-0.11	C34:2	0.07	0.015	0.05	0.025	0.115	-0.099
$C_{39}H_{70}O_6Na$	657.5065	0.03	C36:2	0.14	0.031	0.21	0.077	0.022 [f]	0.143
$C_{47}H_{86}O_6Na$	769.6317	0.97	C44:2	0.09	0.021	0.07	0.050	0.319	-0.064
$C_{49}H_{90}O_6Na$	797.663	0.55	C46:2	0.28	0.067	0.23	0.140	0.353	-0.060
$C_{50}H_{92}O_6Na$	811.6786	-0.02	C47:2	0.09	0.106	0.10	0.183	0.813	0.015
$C_{51}H_{94}O_6Na$	825.6943	0.57	C48:2	0.62	0.123	0.52	0.253	0.245	-0.074
$C_{52}H_{96}O_6Na$	839.7099	1.21	C49:2	0.15	0.117	0.15	0.218	0.974	-0.002
$C_{53}H_{98}O_6Na$	853.7256	0.66	C50:2	5.04	0.181	4.08	0.318	0.000 [f]	-0.242
$C_{54}H_{100}O_6Na$	867.7412	1	C51:2	0.55	0.052	0.40	0.096	0.000	-0.198
$C_{55}H_{102}O_6Na$	881.7569	0.74	C52:2	31.94	0.933	31.47	0.951	0.287	-0.068
$C_{56}H_{104}O_6Na$	895.7725	1.09	C53:2	0.65	0.025	0.53	0.064	0.000 [f]	-0.213

$C_{57}H_{106}O_6Na$	909.7882	1.45	C54:2	4.42	0.207	4.31	1.529	0.816	-0.015
Diunsaturated				**44.04**	**0.686**	**42.12**	**1.125**	**0.000**	
$C_{34}H_{58}O_6Na$	585.4126	-0.57	C31:3	0.04	0.024	0.03	0.033	0.363	-0.058
$C_{39}H_{68}O_6Na$	655.4908	0.04	C36:3	0.09	0.022	0.10	0.043	0.945	0.004
$C_{49}H_{88}O_6Na$	795.6473	0.23	C46:3	0.08	0.020	0.05	0.037	0.031	-0.131
$C_{51}H_{92}O_6Na$	823.6786	0.75	C48:3	0.15	0.052	0.12	0.096	0.352	-0.060
$C_{53}H_{96}O_6Na$	851.7099	0.75	C50:3	1.35	0.075	0.98	0.125	0.000	-0.241
$C_{54}H_{98}O_6Na$	865.7256	0.77	C51:3	0.21	0.034	0.16	0.071	0.077	-0.110
$C_{55}H_{100}O_6Na$	879.7412	0.37	C52:3	13.07	0.513	10.99	0.646	0.000	-0.240
$C_{56}H_{102}O_6Na$	893.7569	0.4	C53:3	0.59	0.028	0.52	0.071	0.008 [f]	-0.164
$C_{57}H_{104}O_6Na$	907.7725	0.07	C54:3	10.08	0.353	14.63	1.288	0.000 [f]	0.253
$C_{58}H_{106}O_6Na$	921.7882	1.16	C55:3	0.11	0.011	0.11	0.019	0.331	0.062
$C_{59}H_{108}O_6Na$	935.8038	0.82	C56:3	0.54	0.039	0.77	0.095	0.000 [f]	0.234
Triunsaturated				**26.32**	**0.797**	**28.45**	**1.502**	**0.001**	
$C_{53}H_{94}O_6Na$	849.6943	0.7	C50:4	0.18	0.017	0.12	0.030	0.000	-0.219
$C_{55}H_{98}O_6Na$	877.7256	0.7	C52:4	2.38	0.159	1.71	0.146	0.000	-0.250
$C_{56}H_{100}O_6Na$	891.7412	-0.14	C53:4	0.19	0.013	0.15	0.022	0.000	-0.208
$C_{57}H_{102}O_6Na$	905.7569	0.14	C54:4	5.04	0.351	6.56	0.722	0.000 [f]	0.222
$C_{58}H_{104}O_6Na$	919.7725	0.95	C55:4	0.06	0.014	0.05	0.013	0.203	-0.081
$C_{59}H_{106}O_6Na$	933.7882	0.88	C56:4	0.48	0.047	0.59	0.083	0.003 [f]	0.174
Tetraunsaturated				**8.33**	**0.556**	**9.18**	**0.870**	**0.018**	
$C_{55}H_{96}O_6Na$	875.7099	0.69	C52:5	0.25	0.021	0.17	0.019	0.000	-0.248
$C_{57}H_{100}O_6Na$	903.7412	0.18	C54:5	1.42	0.143	1.56	0.205	0.100	0.103
$C_{59}H_{104}O_6Na$	931.7725	0.32	C56:5	0.35	0.037	0.36	0.055	0.445	0.049
Pentaunsaturated				**2.03**	**0.194**	**2.10**	**0.267**	**0.509**	
$C_{57}H_{98}O_6Na$	901.7256	-0.83	C54:6	0.24	0.030	0.23	0.033	0.514	-0.042
$C_{59}H_{102}O_6Na$	929.7569	-1.33	C56:6	0.07	0.092	0.14	0.068	0.085	0.107
Hexaunsaturated				**0.31**	**0.105**	**0.37**	**0.099**	**0.234**	

[a] Mean mass error expressed as ppm.

[b] CN/DB, carbon number/double bonds of the TAG acyl chains.

[c] Mean of ion normalized abundances; 10 samples per group were determined in duplicate, the averages of the duplicates were used in the calculations.

[d] P values were obtained by Student's t-test (IBM SPSS statistics v.20), assuming equality of variances according to Levene's test ($p>0.05$).

[e] Loading in the first factor of the PLS-DA model developed with TAG data (SIMCA, Umetrics AB).

[f] P values were obtained by Student's t-test, assuming non-equal variance according to Levene's test ($p<0.05$).

Highlights

New analytical approaches applied to lipid fraction were assayed to authenticate Iberian dry-cured ham

Chemometrics was applied to analytical data to discriminate Iberian dry-cured ham categories

Triacylglycerol profile determined by UHRMS is a promising approach for discrimination

Fingerprint provided by thermograms from DSC is a promising approach for discrimination

These approaches may prove extremely useful to authenticate many foods containing high to moderate amounts of lipids

Tables

Table 1. Fatty acid composition (peak area normalization expressed in %) of *Cebo* and *Bellota* samples.

Fatty acid	*Cebo* (n=10)[a]		*Bellota* (n=10)[a]		p[b]	Loading[c]
	Mean	SD	Mean	SD		
C10:0	0.05	0.004	0.04	0.003	0.000	-0.262
C12:0	0.07	0.004	0.06	0.011	0.009	-0.159
C14:0	1.46	0.060	1.22	0.097	0.000[d]	-0.235
C15:0	0.06	0.006	0.05	0.006	0.000	-0.228
C16:0	23.47	0.521	20.67	0.832	0.000	-0.252
C17:0	0.34	0.028	0.29	0.042	0.003	-0.176
C18:0	10.88	0.504	9.64	0.711	0.000	-0.203
C20:0	0.18	0.017	0.18	0.014	0.913	0.007
C24:0	0.07	0.023	0.04	0.011	0.003[d]	-0.184
SFA	**36.58**	**0.830**	**32.17**	**1.365**	**0.000**	
C16:1n-9	0.34	0.017	0.42	0.021	0.000	0.251
C16:1n-7	2.55	0.177	1.89	0.254	0.000	-0.239
C17:1n-7	0.35	0.029	0.27	0.051	0.000	-0.200
C18:1n-9	44.89	0.437	52.08	1.375	0.000[d]	0.269
C18:1n-7	3.59	0.166	2.74	0.339	0.000[d]	-0.239
C20:1n-9	1.20	0.108	1.36	0.127	0.006	0.164
C24:1n-9	0.07	0.010	0.04	0.015	0.000	-0.201
MUFA	**52.99**	**0.687**	**58.81**	**1.045**	**0.000**	
C18:2n-6	8.40	0.467	7.42	0.412	0.000	-0.212
C20:2n-6	0.56	0.045	0.48	0.050	0.002	-0.180
C20:3n-6	0.07	0.007	0.06	0.008	0.005	-0.168
C20:4n-6	0.12	0.011	0.10	0.014	0.000	-0.205
n-6 PUFA	**9.15**	**0.505**	**8.06**	**0.468**	**0.000**	
C18:3n-3	0.55	0.039	0.45	0.046	0.000	-0.217
C20:3n-3	0.12	0.018	0.10	0.015	0.022	-0.142
C20:5n-3	0.02	0.009	0.02	0.005	0.061	-0.119
n-3 PUFA	**0.69**	**0.047**	**0.56**	**0.059**	**0.000**	
PUFA	**9.84**	**0.550**	**8.62**	**0.519**	**0.000**	
trans 18:1	0.59	0.092	0.40	0.079	0.000	-0.214

Abbreviations: SFA, saturated fatty acids; MUFA, monounsaturated fatty acids; PUFA,

polyunsaturated fatty acids.

[a] 10 samples per group were determined in duplicate, the averages of the duplicates were used in the calculations.

[b] P values were obtained by Student's t-test (IBM SPSS statistics v.20), assuming equality of variances according to Levene's test ($p>0.05$).

[c] Loading in the first factor of the PLS-DA model developed with fatty acid data (SIMCA, Umetrics AB).

[d] P values were obtained by Student's t-test, assuming non-equality of variances according to Levene's test ($p<0.05$).

Table 2. Triacylglycerol (TAG) composition (normalized ion abundances expressed in %) of *Cebo* and *Bellota* samples.

TAG molecular Formula	*m/z* $[M+Na]^+$	Δ (ppm)[a]	CN/DB[b]	*Cebo* (n=10)[c]		*Bellota* (n=10)[c]		*p*[d]	Loading[e]
				Mean	SD	Mean	SD		
$C_{37}H_{70}O_6Na$	633.5065	-0.15	C34:0	0.10	0.021	0.12	0.047	0.144 [f]	0.094
$C_{49}H_{94}O_6Na$	801.6943	1.1	C46:0	0.11	0.092	0.11	0.132	0.866	-0.011
Saturated				**0.21**	**0.102**	**0.23**	**0.158**	**0.781**	
$C_{30}H_{54}O_6Na$	533.3813	-0.67	C27:1	0.04	0.022	0.02	0.023	0.078	-0.110
$C_{36}H_{66}O_6Na$	617.4752	-0.69	C33:1	0.01	0.009	0.05	0.042	0.020 [f]	0.149
$C_{37}H_{68}O_6Na$	631.4908	0.19	C34:1	0.13	0.030	0.15	0.047	0.327	0.063
$C_{39}H_{72}O_6Na$	659.5221	0.37	C36:1	0.09	0.019	0.18	0.064	0.002 [f]	0.187
$C_{45}H_{84}O_6Na$	743.616	1	C42:1	0.05	0.023	0.02	0.040	0.061	-0.116
$C_{47}H_{88}O_6Na$	771.6473	0.8	C44:1	0.13	0.050	0.11	0.099	0.588	-0.035
$C_{49}H_{92}O_6Na$	799.6786	0.91	C46:1	0.25	0.119	0.23	0.213	0.842	-0.013
$C_{50}H_{94}O_6Na$	813.6943	0.71	C47:1	0.12	0.143	0.15	0.241	0.730	0.022
$C_{51}H_{96}O_6Na$	827.7099	0.87	C48:1	0.91	0.129	0.78	0.271	0.202	-0.081
$C_{52}H_{98}O_6Na$	841.7256	0.84	C49:1	0.16	0.098	0.15	0.186	0.922	-0.006
$C_{53}H_{100}O_6Na$	855.7412	1.24	C50:1	4.75	0.235	4.05	0.509	0.001	-0.186
$C_{54}H_{102}O_6Na$	869.7569	1.69	C51:1	0.37	0.051	0.25	0.074	0.000	-0.197
$C_{55}H_{104}O_6Na$	883.7725	1.55	C52:1	11.76	0.717	11.42	1.385	0.000 [f]	-0.043
Monounsaturated				**18.77**	**1.239**	**17.55**	**2.115**	**0.135**	
$C_{37}H_{66}O_6Na$	629.4752	-0.11	C34:2	0.07	0.015	0.05	0.025	0.115	-0.099
$C_{39}H_{70}O_6Na$	657.5065	0.03	C36:2	0.14	0.031	0.21	0.077	0.022 [f]	0.143
$C_{47}H_{86}O_6Na$	769.6317	0.97	C44:2	0.09	0.021	0.07	0.050	0.319	-0.064
$C_{49}H_{90}O_6Na$	797.663	0.55	C46:2	0.28	0.067	0.23	0.140	0.353	-0.060
$C_{50}H_{92}O_6Na$	811.6786	-0.02	C47:2	0.09	0.106	0.10	0.183	0.813	0.015
$C_{51}H_{94}O_6Na$	825.6943	0.57	C48:2	0.62	0.123	0.52	0.253	0.245	-0.074
$C_{52}H_{96}O_6Na$	839.7099	1.21	C49:2	0.15	0.117	0.15	0.218	0.974	-0.002
$C_{53}H_{98}O_6Na$	853.7256	0.66	C50:2	5.04	0.181	4.08	0.318	0.000 [f]	-0.242
$C_{54}H_{100}O_6Na$	867.7412	1	C51:2	0.55	0.052	0.40	0.096	0.000	-0.198
$C_{55}H_{102}O_6Na$	881.7569	0.74	C52:2	31.94	0.933	31.47	0.951	0.287	-0.068
$C_{56}H_{104}O_6Na$	895.7725	1.09	C53:2	0.65	0.025	0.53	0.064	0.000 [f]	-0.213

$C_{57}H_{106}O_6Na$	909.7882	1.45	C54:2	4.42	0.207	4.31	1.529	0.816	-0.015
Diunsaturated				**44.04**	**0.686**	**42.12**	**1.125**	**0.000**	
$C_{34}H_{58}O_6Na$	585.4126	-0.57	C31:3	0.04	0.024	0.03	0.033	0.363	-0.058
$C_{39}H_{68}O_6Na$	655.4908	0.04	C36:3	0.09	0.022	0.10	0.043	0.945	0.004
$C_{49}H_{88}O_6Na$	795.6473	0.23	C46:3	0.08	0.020	0.05	0.037	0.031	-0.131
$C_{51}H_{92}O_6Na$	823.6786	0.75	C48:3	0.15	0.052	0.12	0.096	0.352	-0.060
$C_{53}H_{96}O_6Na$	851.7099	0.75	C50:3	1.35	0.075	0.98	0.125	0.000	-0.241
$C_{54}H_{98}O_6Na$	865.7256	0.77	C51:3	0.21	0.034	0.16	0.071	0.077	-0.110
$C_{55}H_{100}O_6Na$	879.7412	0.37	C52:3	13.07	0.513	10.99	0.646	0.000	-0.240
$C_{56}H_{102}O_6Na$	893.7569	0.4	C53:3	0.59	0.028	0.52	0.071	0.008 [f]	-0.164
$C_{57}H_{104}O_6Na$	907.7725	0.07	C54:3	10.08	0.353	14.63	1.288	0.000 [f]	0.253
$C_{58}H_{106}O_6Na$	921.7882	1.16	C55:3	0.11	0.011	0.11	0.019	0.331	0.062
$C_{59}H_{108}O_6Na$	935.8038	0.82	C56:3	0.54	0.039	0.77	0.095	0.000 [f]	0.234
Triunsaturated				**26.32**	**0.797**	**28.45**	**1.502**	**0.001**	
$C_{53}H_{94}O_6Na$	849.6943	0.7	C50:4	0.18	0.017	0.12	0.030	0.000	-0.219
$C_{55}H_{98}O_6Na$	877.7256	0.7	C52:4	2.38	0.159	1.71	0.146	0.000	-0.250
$C_{56}H_{100}O_6Na$	891.7412	-0.14	C53:4	0.19	0.013	0.15	0.022	0.000	-0.208
$C_{57}H_{102}O_6Na$	905.7569	0.14	C54:4	5.04	0.351	6.56	0.722	0.000 [f]	0.222
$C_{58}H_{104}O_6Na$	919.7725	0.95	C55:4	0.06	0.014	0.05	0.013	0.203	-0.081
$C_{59}H_{106}O_6Na$	933.7882	0.88	C56:4	0.48	0.047	0.59	0.083	0.003 [f]	0.174
Tetraunsaturated				**8.33**	**0.556**	**9.18**	**0.870**	**0.018**	
$C_{55}H_{96}O_6Na$	875.7099	0.69	C52:5	0.25	0.021	0.17	0.019	0.000	-0.248
$C_{57}H_{100}O_6Na$	903.7412	0.18	C54:5	1.42	0.143	1.56	0.205	0.100	0.103
$C_{59}H_{104}O_6Na$	931.7725	0.32	C56:5	0.35	0.037	0.36	0.055	0.445	0.049
Pentaunsaturated				**2.03**	**0.194**	**2.10**	**0.267**	**0.509**	
$C_{57}H_{98}O_6Na$	901.7256	-0.83	C54:6	0.24	0.030	0.23	0.033	0.514	-0.042
$C_{59}H_{102}O_6Na$	929.7569	-1.33	C56:6	0.07	0.092	0.14	0.068	0.085	0.107
Hexaunsaturated				**0.31**	**0.105**	**0.37**	**0.099**	**0.234**	

[a] Mean mass error expressed as ppm.

[b] CN/DB, carbon number/double bonds of the TAG acyl chains.

[c] Mean of ion normalized abundances; 10 samples per group were determined in duplicate, the averages of the duplicates were used in the calculations.

[d] P values were obtained by Student's t-test (IBM SPSS statistics v.20), assuming equality of variances according to Levene's test ($p>0.05$).

[e] Loading in the first factor of the PLS-DA model developed with TAG data (SIMCA, Umetrics AB).

[f] P values were obtained by Student's t-test, assuming non-equal variance according to Levene's test ($p<0.05$).

Figures, color version

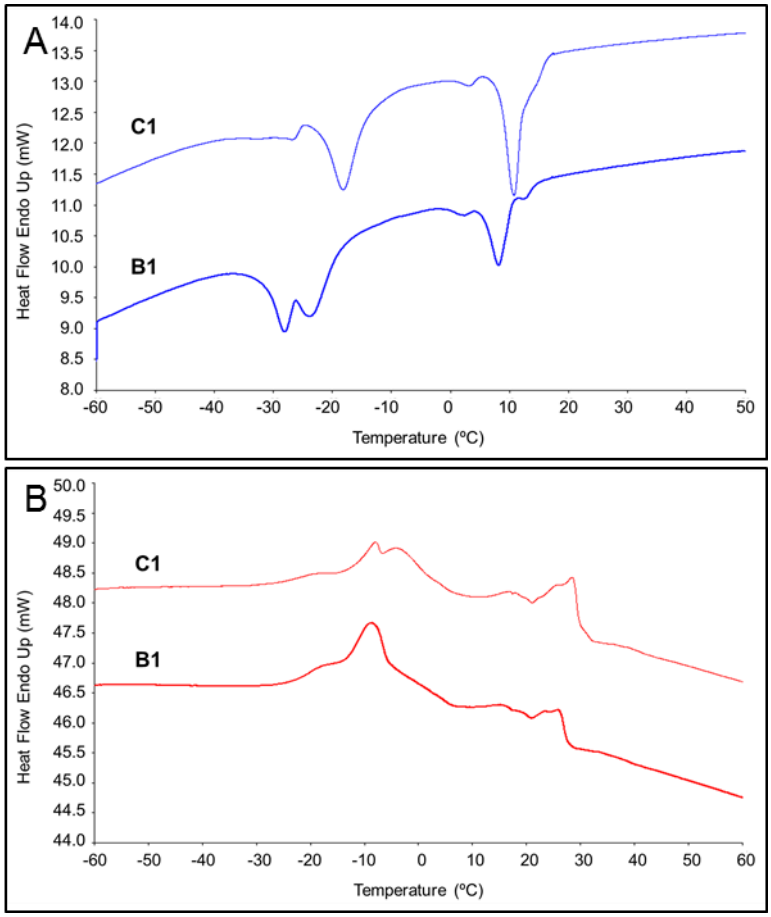

Fig. 1. Typical DSC thermograms of *Cebo* (sample C1) and *Bellota* (sample B1) samples obtained when cooled and heated at 2ºC·min^{-1}. A) DSC cooling curves. B) DSC heating curves.

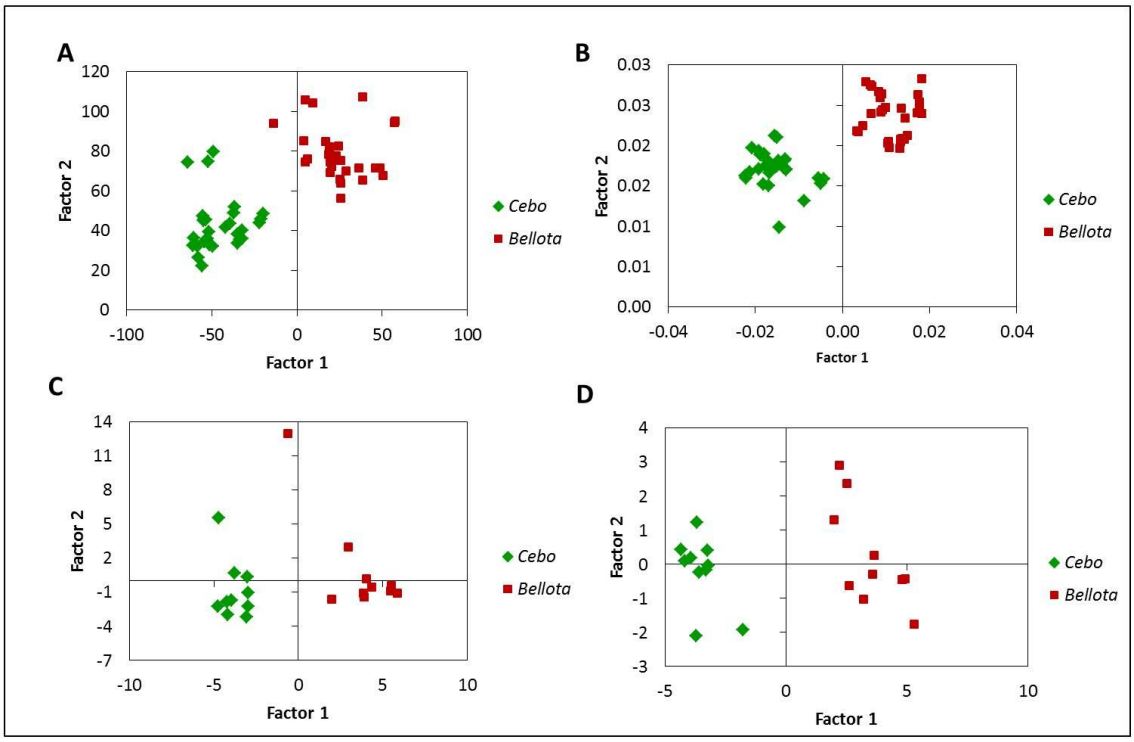

Fig. 2. PLS-DA scores plot: first two factors of the PLS-DA models based on (A) the cooling thermogram (from 25ºC to -45ºC; data correspond to 1st derivative and scaling of variables to unit variance, 3 measurements per sample); (B) heating thermogram (from -30ºC to 40ºC; data correspond to 1st derivative of variables, 3 measurements per sample); (C) triacylglycerol composition by UHRMS (data correspond to variable centering and scaling to unit variance, averages of two determinations per sample); and (D) fatty acid composition (data correspond to variable centering and scaling to unit variance, averages of two determinations per sample).

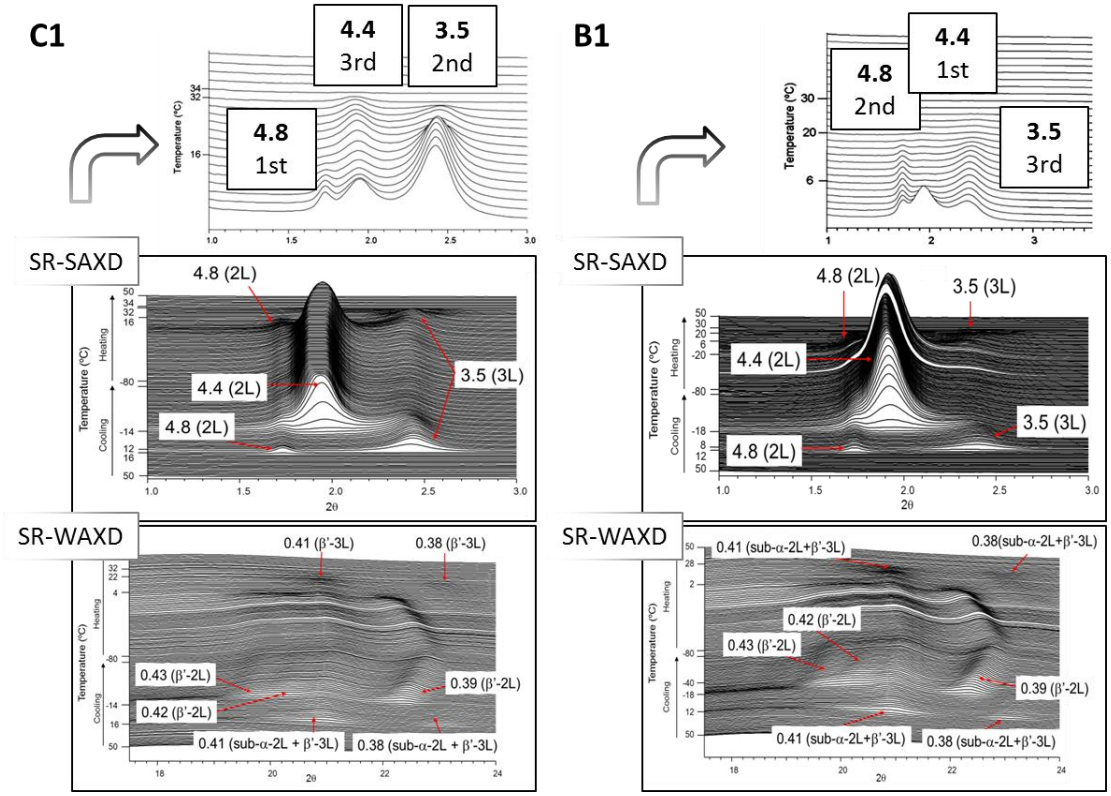

Fig. 3. SR-SAXD and SR-WAXD patterns of C1 and B1 samples.

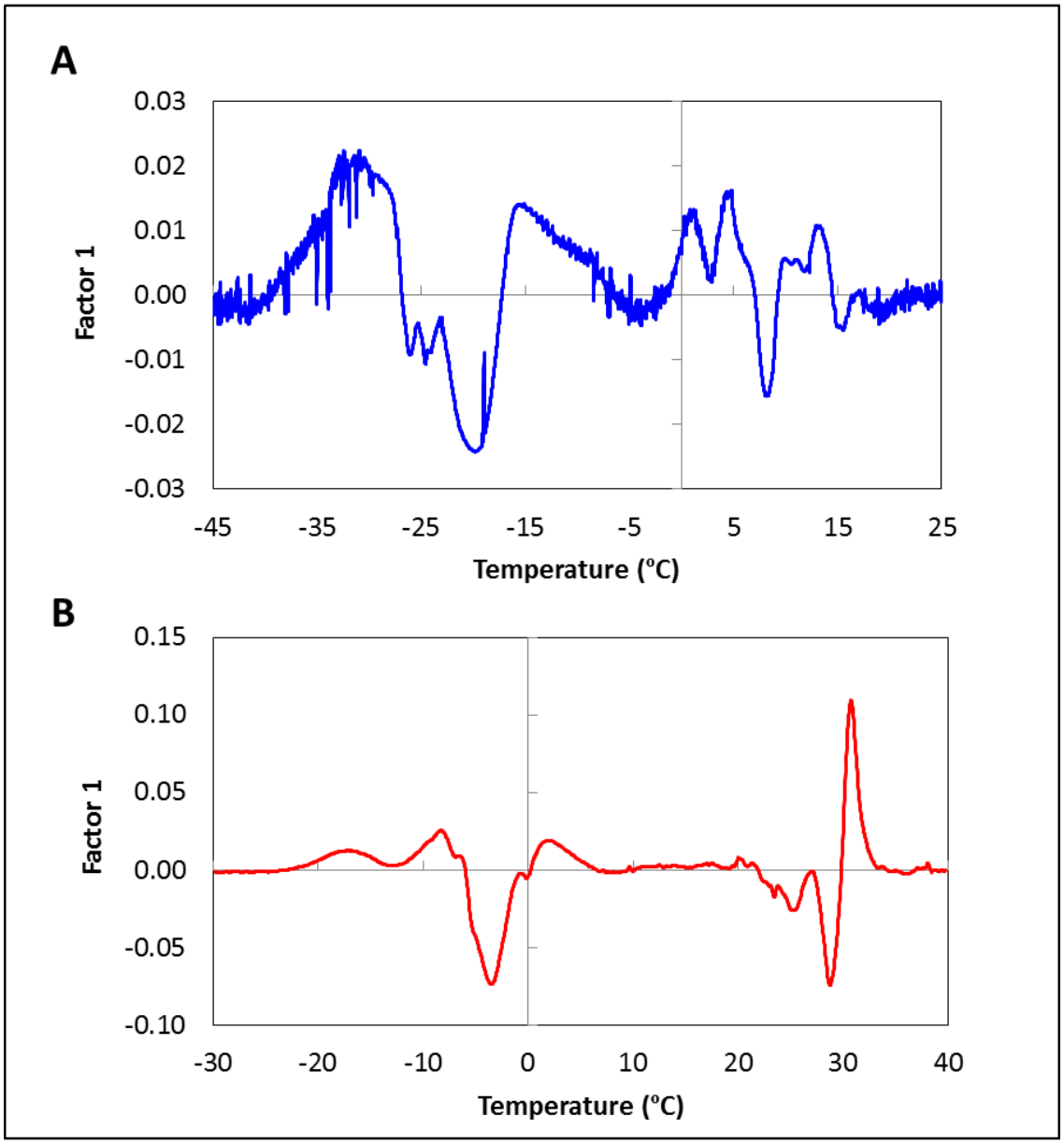

Fig. 4. PLS-DA loadings plot: first factors of the models based on (A) the cooling thermogram (from 25ºC to -45ºC; data correspond to 1st derivative and scaling of variables to unit variance); and (B) heating thermogram (from -30ºC to 40ºC; data correspond to 1st derivative of variables).

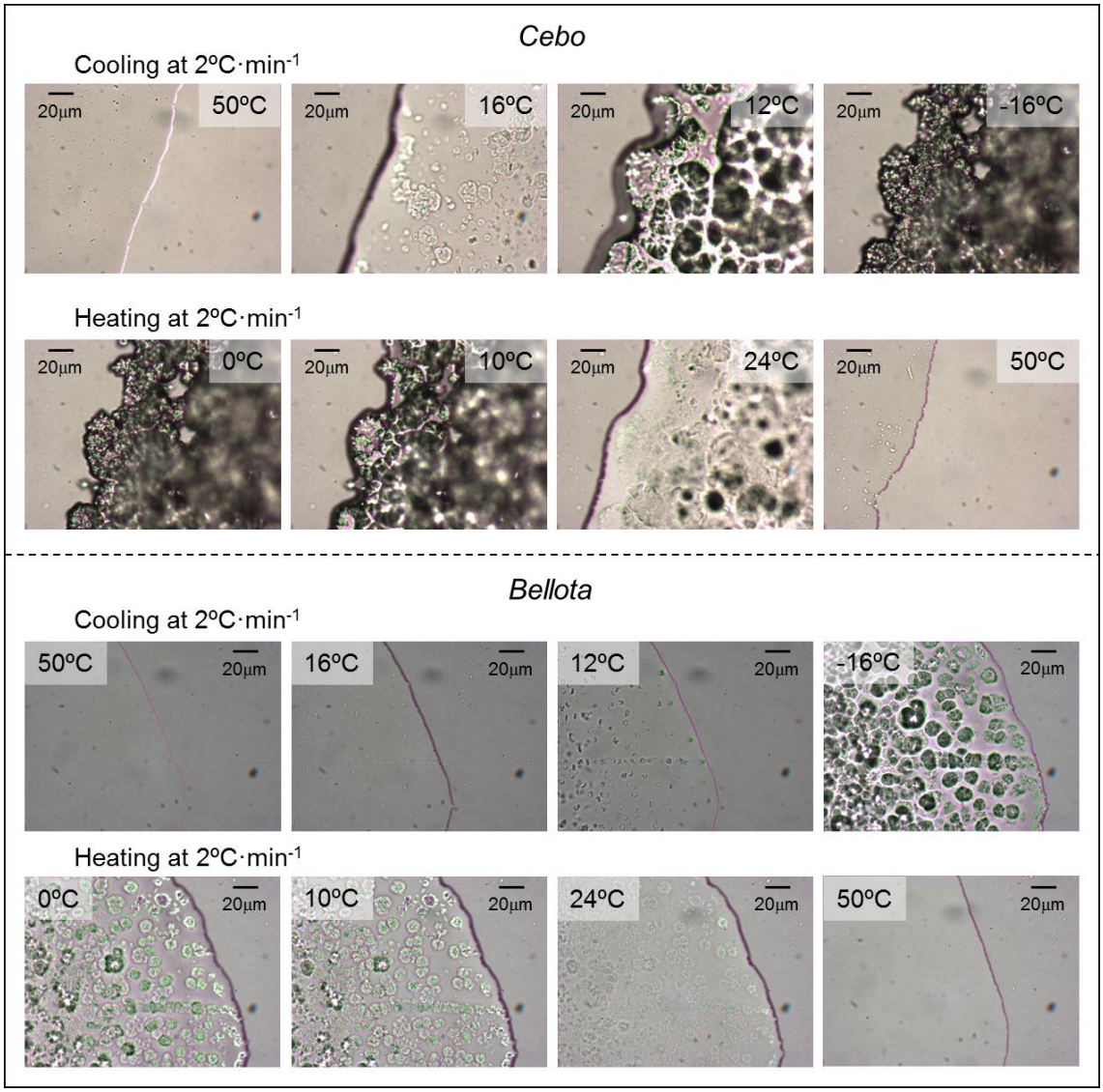

Fig. 5. Thermo-optical polarized microscopy images obtained when *Cebo* and *Bellota* samples were cooled and heated at 2ºC·min^{-1}.

Figures, black and white version

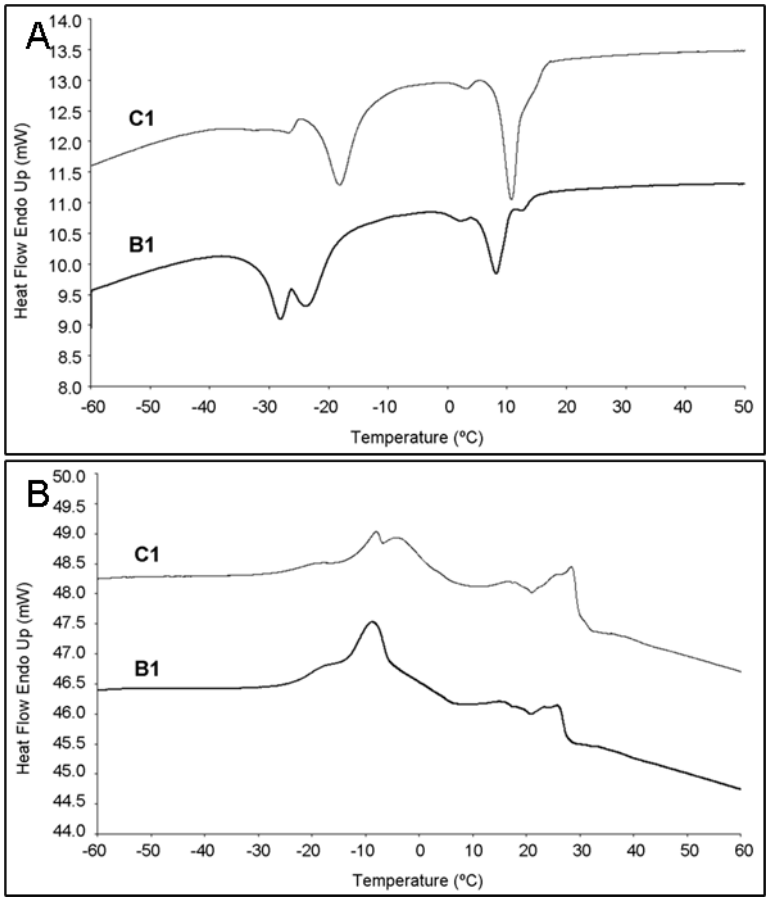

Fig. 1. Typical DSC thermograms of *Cebo* (sample C1) and *Bellota* (sample B1) samples obtained when cooled and heated at 2ºC·min^{-1}. A) DSC cooling curves. B) DSC heating curves.

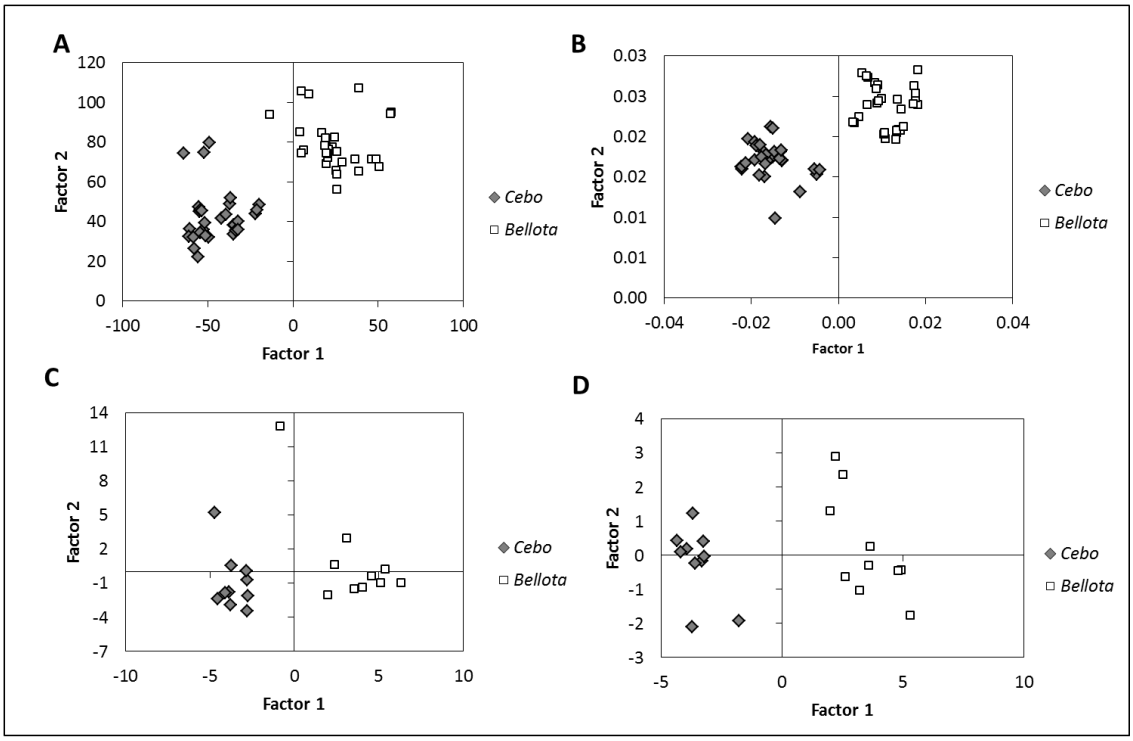

Fig. 2. PLS-DA scores plot: first two factors of the PLS-DA models based on (A) the cooling thermogram (from 25ºC to -45ºC; data correspond to 1st derivative and scaling of variables to unit variance, 3 measurements per sample); (B) heating thermogram (from -30ºC to 40ºC; data correspond to 1st derivative of variables, 3 measurements per sample); (C) triacylglycerol composition by UHRMS (data correspond to variable centering and scaling to unit variance, averages of two determinations per sample); and (D) fatty acid composition (data correspond to variable centering and scaling to unit variance, averages of two determinations per sample).

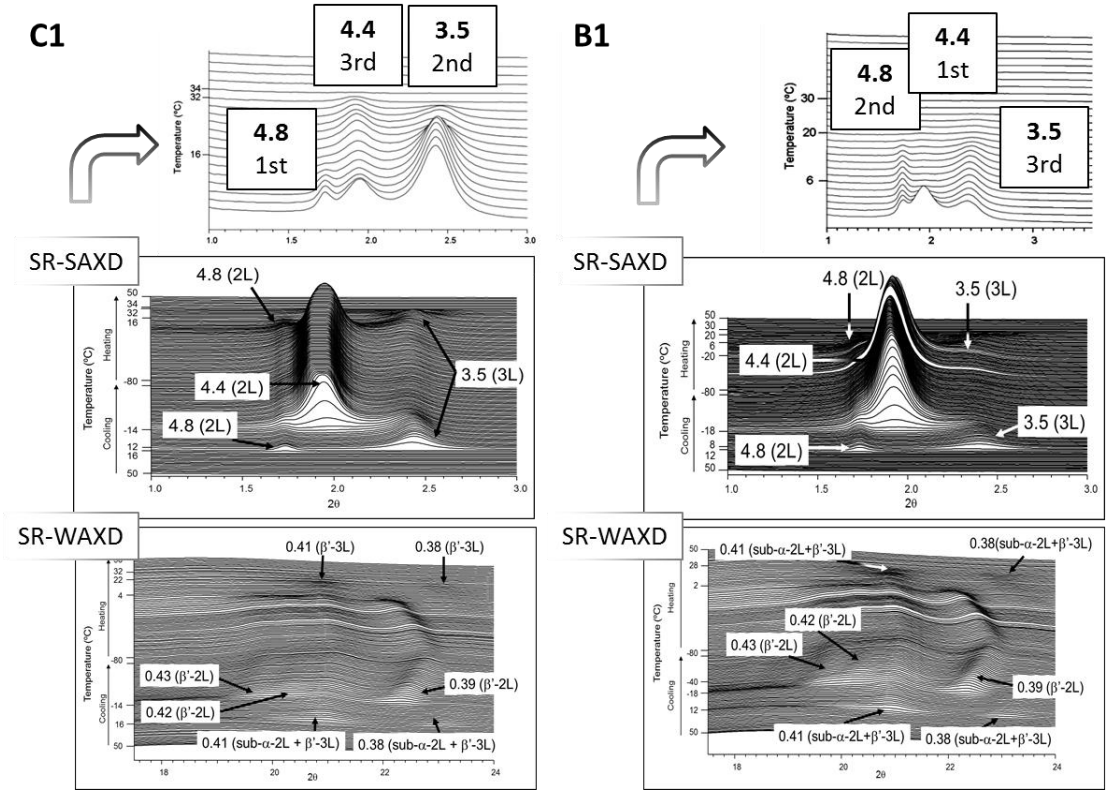

Fig. 3. SR-SAXD and SR-WAXD patterns of C1 and B1 samples.

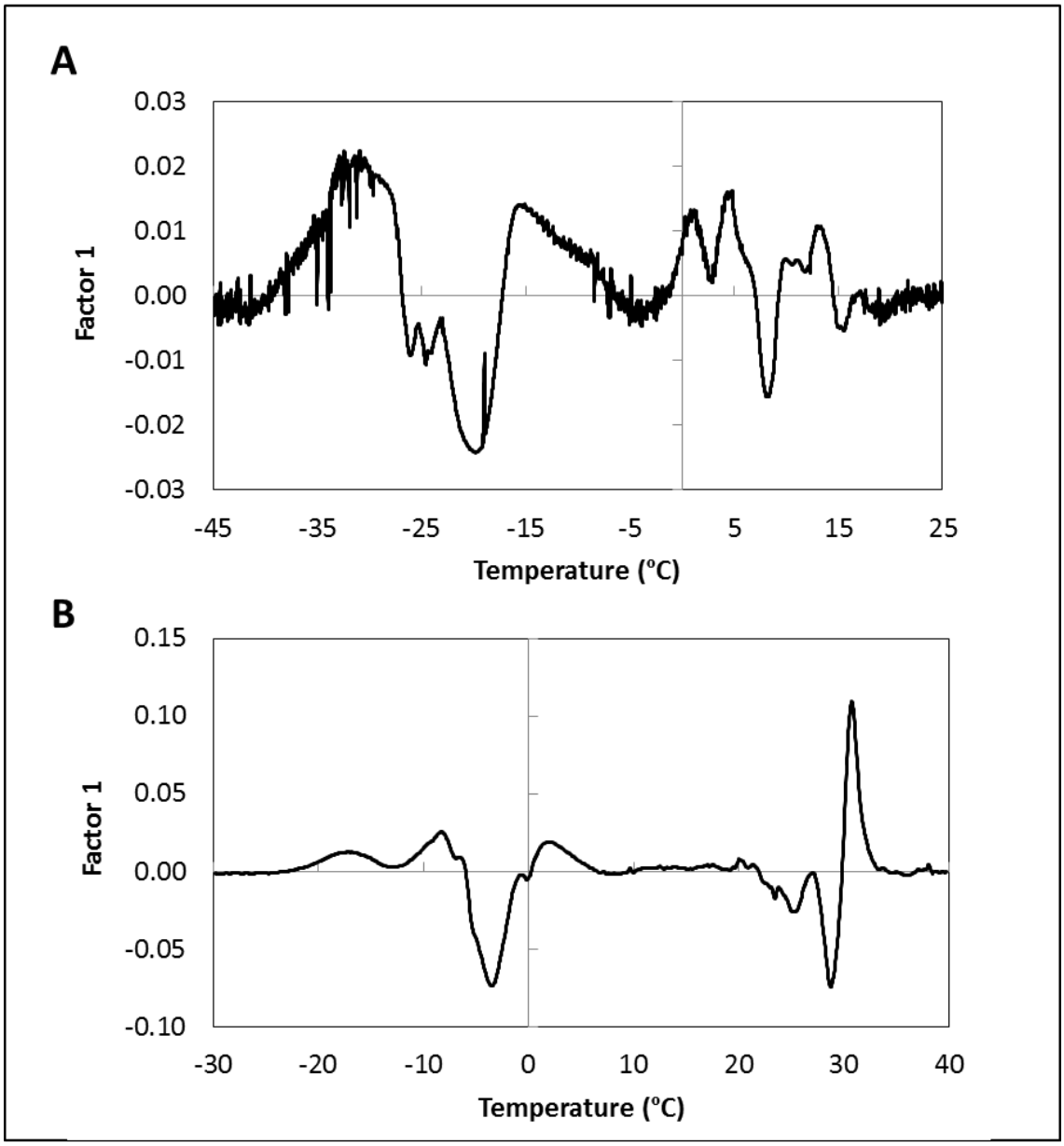

Fig. 4. PLS-DA loadings plot: first factors of the models based on (A) the cooling thermogram (from 25ºC to -45ºC; data correspond to 1st derivative and scaling of variables to unit variance); and (B) heating thermogram (from -30ºC to 40ºC; data correspond to 1st derivative of variables).

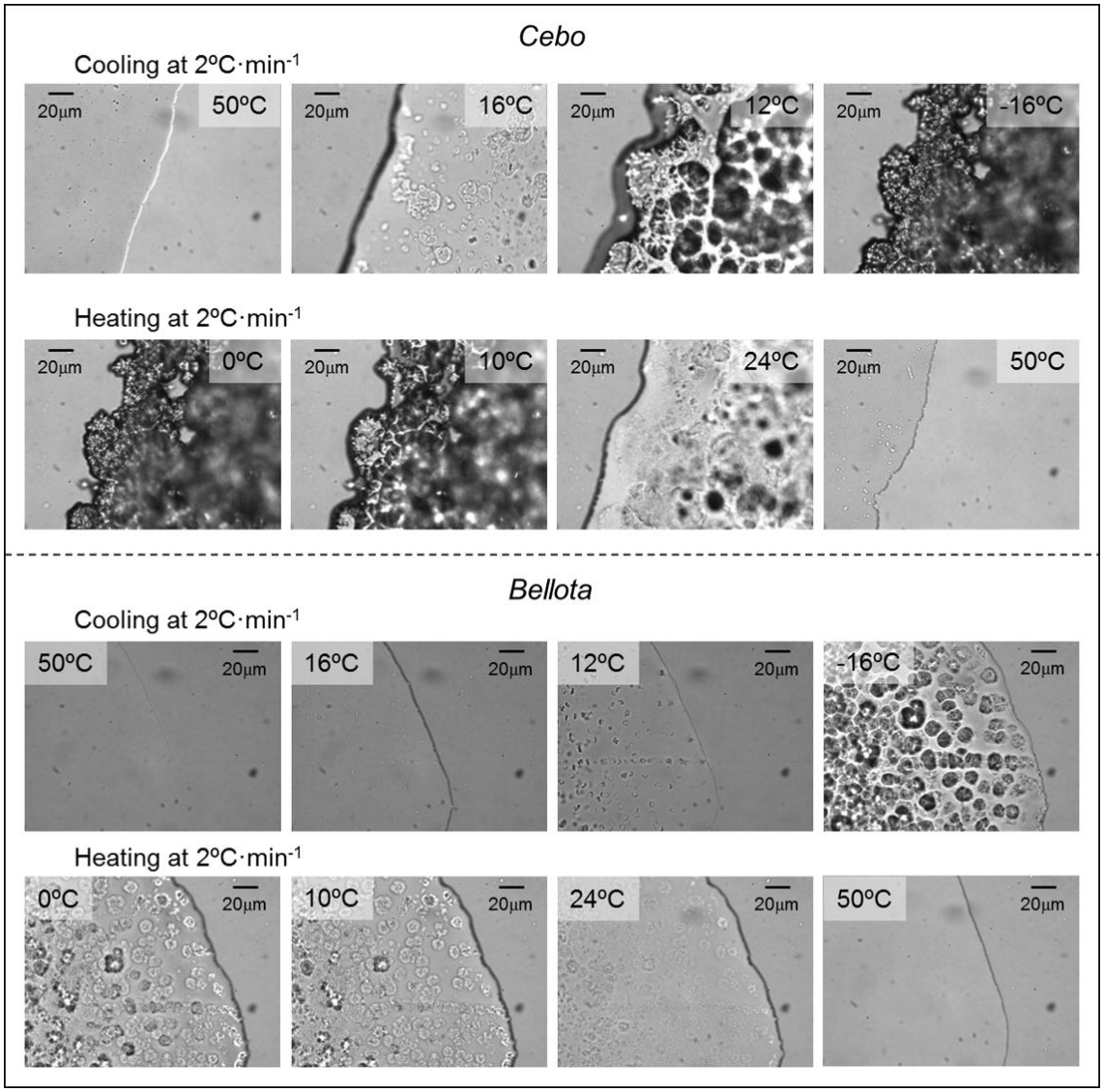

Fig. 5. Thermo-optical polarized microscopy images obtained when *Cebo* and *Bellota* samples were cooled and heated at 2ºC·min^{-1}.